

# Cell-compatible array of three-dimensional tip electrodes for the detection of nitric oxide release

Sonnur Isik<sup>a</sup>, Luca Berdondini<sup>b</sup>, Joshua Oni<sup>a</sup>, Andrea Blöchl<sup>c</sup>,  
Milena Koudelka-Hep<sup>b</sup>, Wolfgang Schuhmann<sup>a,\*</sup>

<sup>a</sup> *Anal. Chem., Elektroanalytik and Sensorik, Ruhr Universität Bochum, Universitätsstr. 150, D-44780 Bochum, Germany*

<sup>b</sup> *Institute of Microtechnology, Université Neuchâtel, CH-2000 Neuchâtel, Switzerland*

<sup>c</sup> *Lehrstuhl für Molekulare Neurobiochemie, Ruhr Universität Bochum, Universitätsstr. 150, D-44780 Bochum, Germany*

## Abstract

An array of electrodes on which cells could be grown directly was fabricated using silicon anisotropic etching and a thick-photoresist process and employed for the detection of nitric oxide (NO) released from a population of adherently growing human umbilical vein endothelial cells (HUVEC). The electrodes are tip-shaped and are 40  $\mu\text{m}$  high of which only the top 15  $\mu\text{m}$  are exposed Pt-tips. After electrochemical induced modification of the exposed Pt tips using Ni phthalocyanine the individual addressable electrode tips were sensitive and selective for the detection of NO at an applied constant potential of 750 mV. The silicon nitride insulation of the lower part of the tip electrodes prevented the death of the cells upon the application of the working potential at which NO was detected. It also helped to avoid the perturbation of the integrity of the sensing chemistry imparted on the electrode surface that could have resulted from the contact of the adherently growing cells with the active electrode surface. The release of nitric oxide from HUVEC was successfully monitored with different numbers of tip electrodes simultaneously connected as combined working electrode.

*Keywords:* Nitric oxide; Array of electrodes; Microfabrication; Modified electrodes; Endothelial cells

## 1. Introduction

Electrochemical techniques have been identified as the methods of choice for the detection and quantification of redox active biological species because of their simplicity, high sensitivity, high speed and selectivity (Ciszewski and Milczarek, 2004; Xian et al., 1999, 2000; Wightman and Michael, 1999; Raveh et al., 1997; Taha, 2004). However, the success of such detections depends to a large extent on the electrodes employed. Thus the process of electrode design, fabrication, electrode surface modification with electroactive catalysts, where applicable (Durst et al., 1997; Elliot and Murray, 1976; Kissinger and Heineman, 1996; Bard, 1983; Brett and Brett, 1980), and the geometry of the electrode,

play significant roles in determining the magnitude of the current signals obtainable from a particular redox active biological species. For example, cylindrical electrodes (Privat et al., 1997; Malinski and Taha, 1992; Bedioui et al., 1996) are more commonly used for the detection of species in biological medium because of the larger surface area and consequently the higher current signal obtained as compared to disc-shaped electrodes.

Array of electrodes are particularly interesting for the detection and analysis of species of biological interest not only because the current signals obtained are additive (i.e. the overall signal is a sum of the individual current signals from each electrode in the array) thereby increasing the sensitivity (Fletcher and Horne, 1999), but also useful in cases where the simultaneous multi-analyte detection is intended. For simultaneous multi-analyte detection, the electrodes in the array are normally individually addressable to pave the way for

\* Corresponding author. Tel.: +49 234 322 6200; fax: +49 234 321 4683.  
E-mail address: wolfgang.schuhmann@rub.de (W. Schuhmann).

fine-tuning the sensitivity and selectivity of each electrode in the array to a particular analyte (Oni et al., 2004; Castillo et al., 2004).

The development of electrodes on which cells could be grown directly is a major step towards achieving the goal of obtaining electrodes for direct application in biological environments. Recent attempts at growing NO-releasing cells on the surface of electrode arrays were successful, but the high working potential for the detection of NO release led to the death of the cells making it difficult, or better, impossible to detect NO release from the cells (Oni et al., 2004).

In this study, an array of Pt-tip microelectrodes was fabricated using silicon anisotropic etching and a thick-photoresist process, allowing cells to be grown in the “valleys” between the electrodes. It is only the upper part of the tip that is (conducting), the rest of the structure is insulated. The growth of cells on the “valleys” prevented a direct contact of cells with the electroactive tip of the spike, thereby avoiding cell death and makes the detection of the release of NO from the cells possible following stimulation with the appropriate agent.

## 2. Materials and methods

### 2.1. Chemicals

Hank’s buffer (pH 7.4) was used in this study. It was prepared from NaCl, KCl,  $\text{NaH}_2\text{PO}_4$ ,  $\text{MgCl}_2$ ,  $\text{CaCl}_2$ ,  $\text{NaHCO}_3$ , glucose, HEPES buffer (all from Riedel de-Haen, Seelze, Germany), arginine (from Sigma, Steinheim, Germany). Nickel tetrasulfonate phthalocyanine tetrasodium salt, KOH, HF,  $N_\omega$ -nitro-L-arginine methyl ester (L-NAME, a nitric oxide synthase inhibitor) and bradykinin were purchased from

Aldrich (Steinheim, Germany). Silicon wafers were obtained from Wacker Siltronic (Burghausen, Germany).

### 2.2. Electrode array preparation

The fabrication process was described in detail elsewhere (Thiébaud et al., 1999). Briefly, the silicon tips are etched in KOH solution and then the bottom  $\text{Si}_3\text{N}_4$  passivation layer is deposited. This is followed by the evaporation of Ta/Pt layers that are patterned by a lift-off process to define the electrodes, connecting leads and bonding pads. The top passivation layer of silicon nitride is deposited and opened using thick-photoresist technology and plasma etching, exposing the Pt on the upper part of the tip and the bonding pads. A SEM image of one electrode and a schematic representation of its cross-section are shown in Fig. 1 The irregular features at the tip bottom originate from the anisotropic etching process. They consist of superimposed Si/ $\text{Si}_3\text{N}_4$ /Pt/ $\text{Si}_3\text{N}_4$  layers.

### 2.3. Electrode surface modification

The sensitivity of the electrode array towards nitric oxide was improved by modification with nickel tetrasulfonate phthalocyanine tetrasodium salt, a well established electrocatalyst for the oxidation of nitric oxide (Pereira-Rodrigues et al., 2002; Pailleret et al., 2003).

### 2.4. Instrumentation

Petite ampere potentiostats (BAS Instruments, West Lafayette, USA) were used for the amperometric detection of nitric oxide released by adherently growing HUVEC at a constant working potential of 750 mV versus Ag|AgCl.

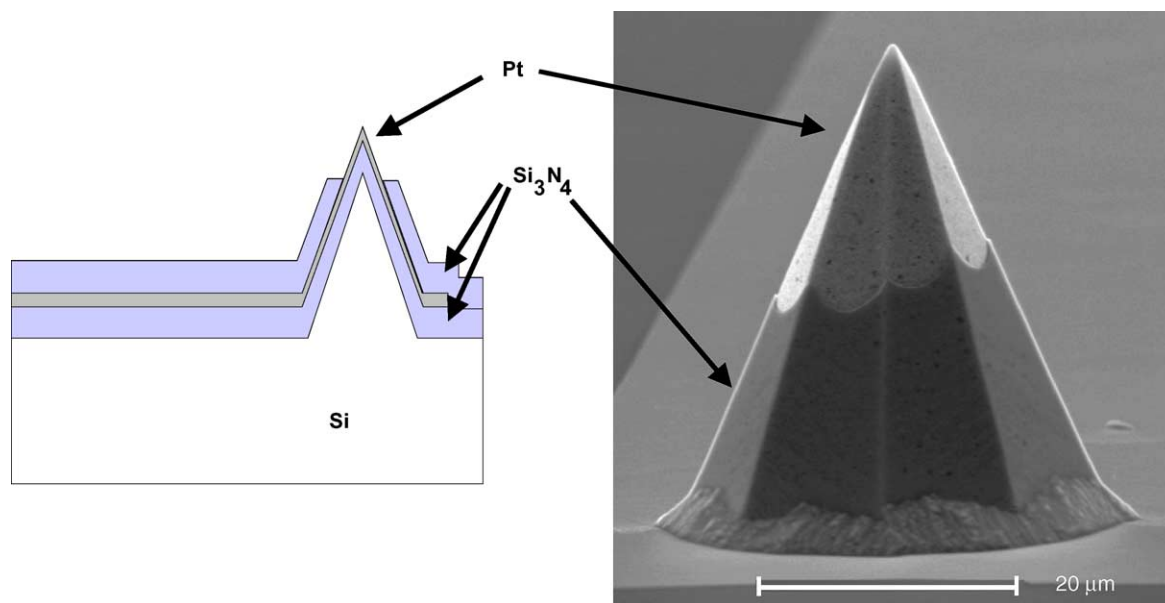


Fig. 1. Scanning electron microscope image of one tip electrode of an array and a schematic representation of its cross-section.

### 2.5. Detection of nitric oxide release from cells

Human umbilical vein endothelial cells (HUVEC) were plated on the array chips in a density of  $2 \times 10^5$  cells per electrode array in RPM-1641, supplemented with 10% foetal calf serum at 37 °C in 10% CO<sub>2</sub> atmosphere. The electrode array was withdrawn from the incubator and the growth medium was carefully replaced with Hank's buffer solution, pH 7.4. Then the electrodes were connected to petite ampere potentiostats and a potential of 750 mV was applied to the electrodes. When a stable background current was obtained, the release of nitric oxide was stimulated by the addition of 20 μL bradykinin solution (80 nM). For control experiments, nitric oxide synthase was inhibited by adding *N*<sub>ω</sub>-nitro-L-arginine methyl ester (L-NAME) to the cell culture.

## 3. Results and discussion

### 3.1. Design of the electrode array

Previous work has shown that the prolonged application of a potential of 750 mV to cells grown directly on an array of electrodes led to the death of the cells (Oni et al., 2004). To overcome this problem, cells were then grown on Cellagen<sup>®</sup> membranes that could be inserted into the electrochemical cell in order to avoid the direct contact between the electrode surface and the cells. While this approach prevented cell death as envisaged, it is not a completely satisfactory solution in that the membrane introduced an additional diffusion layer into the path of nitric oxide on its way from the secreting cells to the sensor surface. Thus, the electrode array employed in this study was designed to accommodate the direct growth of cells on the chip surface and concomitantly to allow for an application of the appropriate working potential to the electrode without adversely affecting the cells or without the cells affecting the integrity of the modifier on the electrode surface. Also, additional diffusional problems posed by the introduction of a membrane to the diffusion path of nitric oxide from the NO-releasing cells to the detector can be circumvented.

The individually addressable electrodes of an electrode array have the additional advantage that the individual electrodes can be combined thus allowing to improve the detection limit and the sensitivity of the NO detection. A SEM image of the electrode array is shown in Fig. 2a while a schematic representation of the relative positions of cells grown directly on the chip surface around the tip electrodes and the active surfaces of an individual electrode in the array is shown in Fig. 2b.

Each electrode array consists of 16 individually accessible electrodes arranged in four rows with 14 electrode tips being connected to contact pads on the printed-circuit board on which the chip is glued and packed by means of epoxy glue. The electrodes in each row are 300 μm apart while the rows are 170 μm apart. The wide separation between the electrodes in the rows and columns is to prevent neighboring electrodes

from interfering by diffusive coupling, and to provide ample space for the cells to be grown on the array. The individual electrodes are tip-shaped with a total height of about 40 μm, and the electroactive top part of the tips is about 17 μm long. The “valleys” between the tip-shaped individual electrodes provide enough room for cells to be grown directly around the electrodes (see Fig. 2b).

### 3.2. Cell survival on electrode arrays

It is of utmost importance that the material with which the electrode array was constructed is biocompatible. The biocompatibility of the microelectrode array with cell growth and survival was investigated by seeding the cells and growing them directly on the microelectrode array. Cells were found to grow well on this surface using standard cell viability (apoptosis) tests. Fig. 3 shows optical microscope images of a HUVEC-modified electrode array in bright-field illumination to visualize the tip electrodes (Fig. 3a) and the immunocytochemistry fluorescence image showing the cytoskeleton of the cells after staining with phalloidine (Fig. 3b). Apart from the visible dense population of cells in Fig. 3b, the tips of the individual electrodes can be seen projecting beyond the plane of the cells grown on the wafer. The circle in Fig. 3b is used to mark the tip of an individual electrode.

### 3.3. Electrode surface modification

Due to the low concentration of nitric oxide in biological systems, electrode surface modification for improved sensitivity is required. The electrodes in the array were selectively modified with a well established nitric oxide sensing chemistry (Pereira-Rodrigues et al., 2002; Pailleret et al., 2003) based on the electrochemically induced deposition of nickel tetrasulfonate phthalocyanine tetrasodium salt onto the individual electrode surfaces. The related cyclic voltammetry recorded during the electrochemical deposition of the catalyst layer is shown in Fig. 4a. The formation of a film of this phthalocyanine on the electrode surface is indicated by the appearance and increase in the peak currents of the anodic and cathodic signals at 420 and 580 mV versus Ag|AgCl (Pereira-Rodrigues et al., 2002; Pailleret et al., 2003). The molecular structure of nickel tetrasulfonate phthalocyanine tetrasodium salt is shown as an inset in Fig. 4a.

The modified electrode was characterized by recording its cyclic voltammetry in 5 mM solution of [Ru(NH<sub>3</sub>)<sub>6</sub>]Cl<sub>3</sub> in 0.1 M KCl as electrolyte. The unmodified electrode only showed the redox current due to Ru<sup>3+</sup>/Ru<sup>2+</sup> couple (Fig. 4b, curve i). An additional redox couple, superimposed on Ru<sup>3+</sup>/Ru<sup>2+</sup> was observed on the phthalocyanine modified electrode (Fig. 4b, curve ii), which can be attributed to a difference in the surfaces of the modified and unmodified electrode, largely due to the electrodeposited film of nickel tetrasulfonate phthalocyanine tetrasodium salt. The cyclic voltammogram at the bare electrode tip shows the typical Ru (III)/Ru (II) reduction wave as expected for a microelectrode.

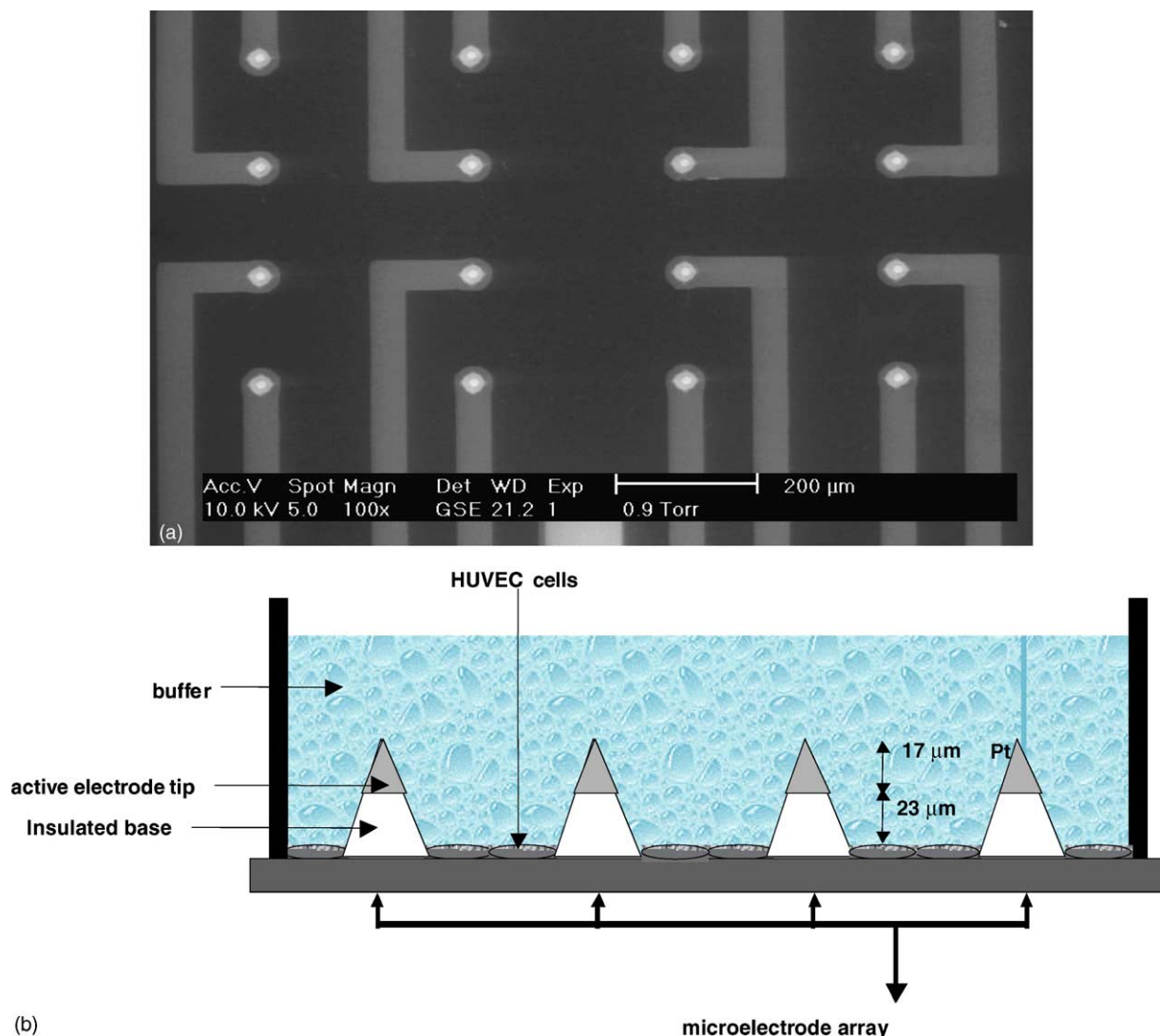


Fig. 2. (a) SEM image of the microstructured electrode array and (b) schematic representation of the relative positions of cells grown directly on the electrode array and the active surfaces of the individual electrode tips in the array.

On the Ni phthalocyanine modified electrode surface this voltammetric wave is nearly unchanged, however, at more negative potentials the Ni redox wave is overlaying on top of the diffusion-limited Ru (III) reduction current. The reduction process in the Ni phthalocyanine layer is obviously slow probably due to counter ions movement while the oxidation wave is fast and the shape representative for an adsorbed or surface bound species.

#### 3.4. Detection of nitric oxide release from adherently growing cells

Having successfully completed the preliminary steps of electrode fabrication, electrode surface modification and growing cells on the electrode array, the release of nitric oxide from endothelial cells grown directly on the chip surface of the electrode array was detected after stimulation with

bradykinin. A constant potential of 750 mV versus Ag|AgCl was applied to the electrodes, a stable background current was established and bradykinin (20 μL, 80 nM) was carefully injected into the droplet of buffer solution (300 μL) above the cells, simultaneously monitoring the changes in current with time. A representative current–time plot recorded is shown in Fig. 5. The traces shown in Fig. 5 were recorded with 14 of the electrodes in the array, which were divided into two parts (a) and (b) with each part consisting of 10 and 4 electrodes, respectively. Each part was connected to a potentiostat using the same reference and counter electrode. Trace (a) corresponds to the current response from 10 combined modified tip electrodes while trace (b) corresponds to the current signals recorded from only 4 combined tips. These current–time traces are similar to those recorded earlier for the detection of nitric oxide from endothelial cells using positioned modified microdisk electrodes (Diab et al., 2003; Oni

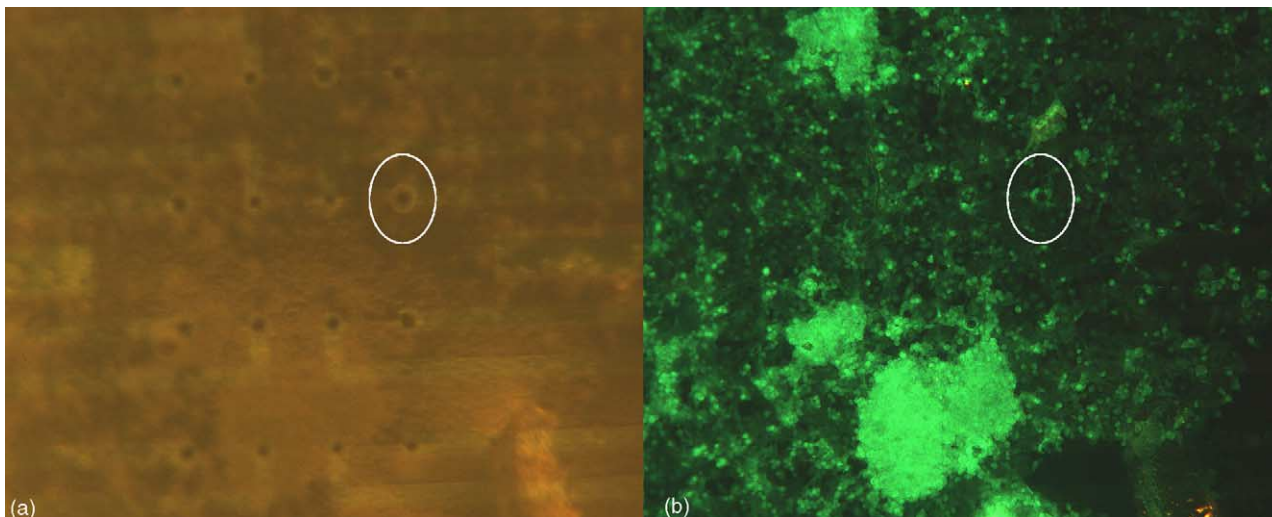


Fig. 3. Immunocytochemistry picture of HUVECs growing on the microarray. The cells were stained with phalloidine in order to visualize the cytoskeleton of the cells. (a) Bright-field microscopy image for visualization of the electrodes and (b) fluorescence microscopy image showing the cytoskeleton of the adherently growing cells. Circles were used to indicate the positions of a particular electrode in both images.

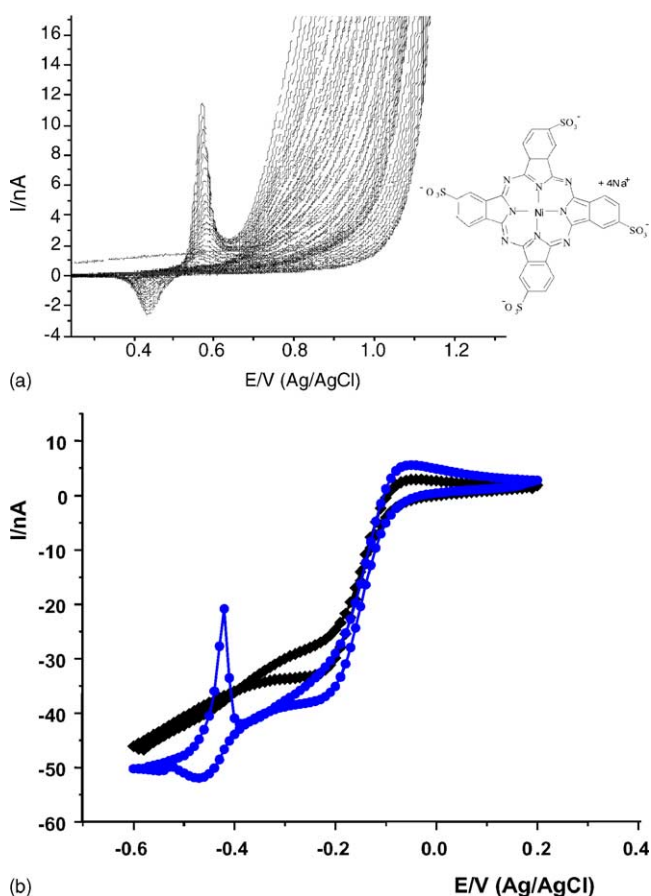


Fig. 4. (a) Repetitive cyclic voltammograms recorded during the electrochemical deposition of nickel tetrasulfonate phthalocyanine tetrasodium salt onto the electrode surface. Its molecular structure is shown as an inset. (b) Cyclic voltammograms of 5 mM solution of  $[\text{Ru}(\text{NH}_3)_6]\text{Cl}_3$  (in 0.1 M KCl as electrolyte) recorded with (i) unmodified Pt microelectrode and (ii) Pt microelectrode on which nickel tetrasulfonate phthalocyanine tetrasodium salt has been deposited.

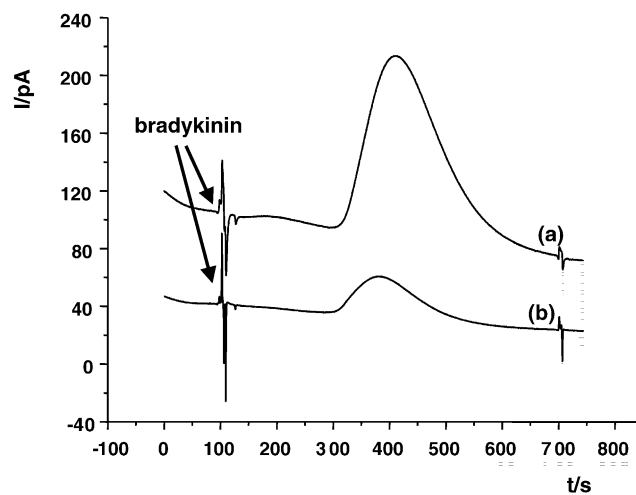


Fig. 5. Current–time plots recorded for the detection of nitric oxide from adherently growing HUVECs after stimulation with bradykinin with (a) 10 and (b) 4 individual electrodes in the array connected to separate potentiostats.

et al., 2003). Obviously, using the modified tip electrodes in the array and the possibility to interconnect variable numbers of the individually addressable electrode tips, the release of nitric oxide from different sites of the chip surface can be explored. As a matter of fact, it would be advantageous to give concentration values for the released NO derived from related calibration curves for NO. However, since the NO concentration at the site of the NO sensors is mainly defined by the distance between the releasing cells and the sensors, possible side reactions like reaction of NO with oxygen, and the establishment of a complex diffusion profile in the vicinity of the cells, it is to our opinion not possible to correlate the observed NO oxidation currents with the actual NO concentration. Even more, the local concentration is correlated with the number of cells releasing NO in the vicinity of the

tip electrodes. Thus, calibration graphs in homogeneous solutions do not give any valid correlation with the complex concentration gradients established after stimulated release of NO from the cells, and hence current–time plots were used to represent the obtained results. However, it is obvious that these current–time plots are concentration dependent, since the current obtained is dependent on the number of connected electrode tips. Future work is directed at developing a suitable multi-potentiostat system with sufficient sensitivity to detect simultaneously the NO release from known areas of the cell-modified chip surface.

Contrary to the earlier observation of cell death made when the working potential of 750 mV was applied to the electrode on which cells were seeded and grown directly, and consequently no detection of products of cellular activity could be made, it was possible to detect the release of nitric oxide from cells grown around the electrode array in this study. This is largely due to the fact that the cells were not grown directly on the active electrode surface within the Debye layer of the potential drop where the applied potential can be passed to the cell, thus potentially causing cell death. Instead, the cells were grown around the insulated base of each electrode in the array with the electroactive tip of the electrode being far above the cell population, thus preventing a direct contact of the tip with cells. Apart from the fact that the electrode array prevented cell death, it also eliminated the problems of NO diffusion introduced by growing cells on a membrane. When cells are grown on a membrane that is located at a certain distance from the electrode, the species released from the cell will not all diffuse downwards towards the electrode surface for detection. But one may argue that the bulk concentration will be the same after a short while. This is only tenable in cases where the species being detected is not sensitive to the ambient environmental conditions. In a case like the detection of nitric oxide, a uniform bulk concentration condition will never be achieved because of its instantaneous reaction with oxygen.

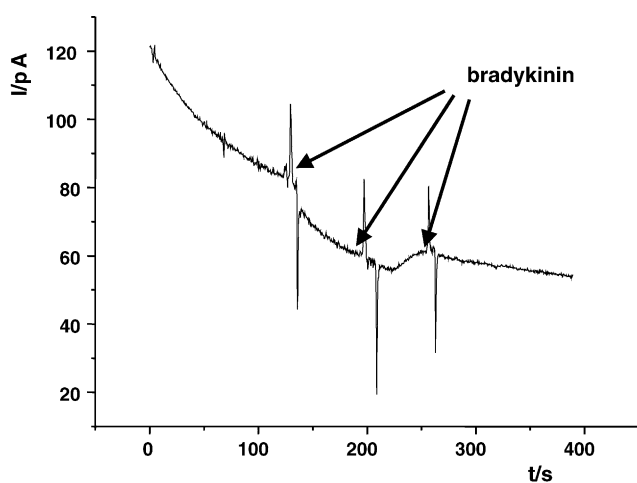


Fig. 6. Current–time plot that showed no nitric oxide release when endothelial cells were first incubated with the nitric oxide synthase inhibitor L-NAME.

Control experiments were performed to confirm that the traces shown in Fig. 5 are due to the detection of the nitric oxide released from the cells, around the electrode, at the electrode surface. The detection experiment was repeated with cells that were incubated with a nitric oxide synthase inhibitor, *N*<sub>ω</sub>-nitro-L-arginine methyl ester (L-NAME). The addition of bradykinin to the cells did not result in measurable current signals as shown in Fig. 6.

This unequivocally confirms that the current signals shown in the traces in Fig. 5 are due to the oxidation of the nitric oxide released by the cells around the electrode array. This arrangement for the detection of species produced due to cellular activities can find widespread application in in situ drug and drug delivery tests on cells, eliminating the often-tedious procedure of complex separation steps before analysis.

#### 4. Conclusion

A microelectrode array consisting of individually addressable tip-shaped electrode with a total height of 40 μm and an exposed Pt surface at the top of the tip with a height of about 15 μm. This electrode configuration allowed for the direct growth of cells on the area occupied by the electrodes without making contacts with the active electrode surface, hence protecting the adherently growing cells from the impact induced by the working potential applied to the tip electrodes. The electrodes of the array were modified with a layer of Ni phthalocyanine following an electrochemically induced deposition scheme, and thus the modified electrodes were subsequently employed to detect the release of nitric oxide from adherently growing endothelial cells upon stimulation with bradykinin. This process has not been possible thus far because of cell death occasioned by a prolonged and continuous application of the rather high working potential of 750 mV to the cells when they are situated directly on the active surface of the electrode. This new electrode design offers much future promise for facilitating drug screening tests.

#### Acknowledgements

The authors thank the European Commission (Cellsens/QLK3-CT-2001-00244) for financial support. LB and MKoH gratefully acknowledge the help of the COMLAB team, Ms S. Pochon and OFES funding (01.0120 CellSens project).

#### References

- Bard, A.J., 1983. Chemically modified electrodes. *J. Chem. Ed.* 60, 303–304.
- Bedioui, F., Trevin, S., Devynck, J., 1996. Chemically modified microelectrodes designed for the electrochemical determination of nitric oxide in biological systems. *Electroanalysis* 8, 1085–1091.
- Brett, C.M.A., Brett, A.M.O., 1980. *Electrochemistry: Principles Methods and Applications*. Wiley, New York.

- Castillo, J., Isik, S., Blöchl, A., Pereira-Rodrigues, N., Bedioui, F., Csöregi, E., Schuhmann, W., Oni, J., 2004. Simultaneous detection of the release of glutamate and nitric oxide from adherently growing cells using an array of glutamate and nitric oxide selective electrodes. *Biosens. Bioelectron.* 20(8) 1559–1565.
- Ciszewski, A., Milczarek, G., 2004. Electrochemical detection of nitric oxide using polymer modified electrodes. *Talanta* 61, 11–26.
- Diab, N., Oni, J., Schulte, A., Radtke, I., Blöchl, A., Schuhmann, W., 2003. Pyrrole functionalised metalloporphyrins as electrocatalysts for the oxidation of nitric oxide. *Talanta* 61, 43–51.
- Durst, R.A., Baumner, A.J., Murray, R.W., Buck, R.P., Andireux, C.P., 1997. Chemically modified electrodes: recommended terminology and definitions. *Pure Appl. Chem.* 69, 1317–1323.
- Elliot, C.M., Murray, R.W., 1976. Chemically modified carbon electrodes. *Anal. Chem.* 48, 1247–1254.
- Fletcher, S., Horne, M.D., 1999. Random assemblies of microelectrodes (RAM<sup>TM</sup> electrodes) for electroanalysis. *Electrochem. Commun.* 1, 502–512.
- Kissinger, P.T., Heineman, W.R. (Eds.), 1996. *Laboratory Techniques for Electroanalytical Chemistry*, 2nd ed. Marcel Dekker, New York.
- Malinski, T., Taha, Z., 1992. Nitric oxide release from a single cell measured in situ by a porphyrinic-based microsensor. *Nature* 358, 676.
- Oni, J., Diab, N., Radtke, I., Schuhmann, W., 2003. Detection of nitric oxide from endothelial cells using Pt microelectrodes modified with a pyrrole-functionalised Mn (II) porphyrin. *Electrochim. Acta* 48, 3349–3354.
- Oni, J., Pailleret, A., Isik, S., Diab, N., Radtke, I., Blöchl, A., Jackson, M., Bedioui, F., Schuhmann, W., 2004. Functionalised array of electrodes for the detection of nitric oxide released by endothelial cells using different NO-sensing chemistries. *Anal. Bioanal. Chem.* 378, 1594–1600.
- Pailleret, A., Oni, J., Reiter, S., Isik, S., Etienne, M., Bedioui, F., Schuhmann, W., 2003. In situ formation and scanning electrochemical microscopy assisted positioning of NO-sensors above human umbilical vein endothelial cells for the detection of nitric oxide release. *Electrochem. Commun.* 5, 847–852.
- Pereira-Rodrigues, N., Albin, V., Koudelka-Hep, M., Auger, V., Pailleret, A., Bedioui, F., 2002. Nickel tetrasulfonated phthalocyanine based platinum microelectrode array for nitric oxide oxidation. *Electrochem. Commun.* 4, 922–927.
- Privat, C., Trevin, S., Bedioui, F., Devynck, J., 1997. Direct electrochemical characterisation of superoxide anion production and its reactivity towards nitric oxide. *J. Electroanal. Chem.* 346, 261–265.
- Raveh, O., Peleg, N., Betleheim, A., Silberman, I., Rishpon, J., 1997. Detection of nitric oxide production in melanoma cells using an amperometric nitric oxide sensor. *Bioelectrochem. Bioenerg.* 43, 19–25.
- Taha, Z.H., 2004. Nitric oxide measurements in biological samples. *Talanta* 61, 3–10.
- Thiébaud, P., Beuret, C., Koudelka-Hep, M., Bove, M., Martinoia, S., Grattarola, M., Jahnsen, H., Rebaudo, R., Balestrino, M., Zimmer, J., Dupont, Y., 1999. An array of Pt-tip microelectrodes for extracellular monitoring of activity of brain slices. *Biosens. Bioelectron.* 14, 61–65.
- Wightman, R.M., Michael, J.D., 1999. Electrochemical monitoring of biogenic amine neurotransmission in real time. *J. Pharm. Biomed. Anal.* 19, 33–46.
- Xian, Y., Xue, J., Zhang, S., Yin, X., Jin, L., 1999. An Ni(chitin)<sub>2</sub> modified nitric oxide microsensor. *Fresenius J. Anal. Chem.* 365, 587–591.
- Xian, Y., Zhang, W., Xue, J., Ying, X., Jin, L., 2000. Direct measurement of nitric oxide release from the rat hippocampus. *Anal. Chim. Acta* 415, 127–133.